

Performance of Optimized Scheduled Follow-up Observations for Geosynchronous Space Objects Using Different Genetic Algorithms

Andreas Hinze

DLR/GSOC, Wessling, Germany

Hauke Fiedler

DLR/GSOC, Wessling, Germany

Thomas Schildknecht

Astronomical Institute, University of Bern, Switzerland

ABSTRACT

The importance of protecting the geosynchronous region from space debris requires continuous monitoring in order to support collision avoidance operations. Accurate orbit information is prerequisite to avoid manoeuvres which might shorten the mission time. To gain this information, follow-up observations are necessary to maintain the accuracy of ephemeris data within certain limits for each catalogued object. To perform these observations in the most efficient way, optimized scheduling is a key element.

In this paper the performance of two optimal scheduling algorithms is compared for an optical telescope network. Both algorithms are based on genetic algorithms and have been utilized to provide optimal solutions for catalogue maintenance. The single-objective algorithm uses the expected information content of a new observation as optimization parameter. The multi-objective algorithm is based on the successful Non-dominated Sorting Genetic Algorithm II (NSGA-II) and uses as further optimization parameter the detection probability given by the pre-estimated magnitude of the object. Both algorithms are introduced in detail and it is shown that the information content utilizing the orbit's covariance and the information gain in an expected update is a useful optimization measure. Since the information content of a follow-up observation depends also on the observation time and oscillates slightly during the night similar information gain values might be reached at different observation epochs. It is demonstrated that an optimized phase angle might not reduce the information content of a follow-up observation substantially. To prove the concept, data of a simulated object catalogue is used to compare the effectiveness of the scheduling algorithms. Finally, first results of the performance of both algorithms using the optical telescope network are shown and analyzed.

1. INTRODUCTION

The space debris population around the Earth is permanently increasing. One of the most important and valuable orbits around the Earth is the Geosynchronous Earth Orbit region (GEO), which is observed by optical observations. During the last years, several survey strategies have been developed to build up a catalogue of space debris objects for characterizing, collision avoidance and to improve the knowledge of the population size (amongst others [4]). For catalogue maintenance, additional observations are necessary to improve the orbit and to keep its accuracy within a given limit. Performing optical observations, the length of the observation night is the most limiting factor. This depends on the location site of the telescope and the season. Providing an optimum coverage of the GEO and to enable a continuous monitoring independent of seasonal limitations, a telescope network distributed around the earth both in the northern and southern hemisphere is required.

The German Space Operations Center (GSOC) builds up a small-aperture robotic telescope network in collaboration with the Astronomical Institute, University of Bern. This telescope network will be used for surveillance observations to build up a space debris catalogue and for tracking observations for catalogue maintenance. More details are given in [5].

In this paper, two algorithms to schedule tracking observations will be shown. If once a determined orbit of a GEO object is good enough to re-observe after several days, this orbit may be added to the catalogue. Simulations showed that after four observation sequences such a "secure" orbit may be determined [10] and an additional follow-up observation may be scheduled after up to one week. Depending on the used telescope and its Field of View (FoV), the position inaccuracy should be less than the half FoV to ensure a successful re-detection. Scheduling of follow-up observations requires knowledge of the target orbit and the available observatories. If the preferred observatory is selected, scheduler usually

take into account the priority of an observation of an object [9] and time constraints. Latter ones have to be optimized corresponding to the reduction of the number of conflicts and to perform as many observations as possible. Since GEO objects could be visible over a longer time span of the observation night, the visibility constraints (e.g. phase angle, background illumination, . . .), which influence the detection probability, are not the only criteria to schedule an observation. The prediction of the effectivity of a future observation depending on the observation geometry and the orbit error covariance may be used to schedule an observation at the most effective time [6][7]. Scheduling of telescopes belongs to a class of NP-hard problems. Consequently, there are no known algorithms guaranteed to give an optimal solution and run in polynomial time. There are several techniques to handle such problems. In this work a single-objective (GA) and a multi-objective genetic algorithm (MOGA) are introduced and simulations are used to show and compare the performance of both algorithms.

2. METHODS

2.1. Information content

The advantages using a telescope network are the possibilities to perform more observations and to have more flexibility to schedule them as opposed to a single telescope. This allows to observe each object more often and to schedule observations at the most effective way. The effectiveness depends on the sensor-target geometry and therefore on the selected station and the observation time as well as on the uncertainty of the catalogued orbit.

The uncertainty of a catalogued orbit is given by the orbit error covariance matrix P . Furthermore, the observation geometry is given by the matrix H which consists of the partial derivatives of the observations with respect to the orbit state.

$$H = \frac{\partial h(x)}{\partial x} \quad (1)$$

Using the equations of the Kalman filter for measurement update

$$K = P^- H^T (W^{-1} + H P^- H^T)^{-1} \quad (2)$$

$$P^+ = (I - KH) P^- \quad (3)$$

where K is the Kalman gain, P^- the propagated covariance matrix to the epoch of the observation, W the weighting matrix which is in this case the inverse of the observation error matrix and P^+ the updated orbit error covariance matrix a method is given which connects the three mentioned dependencies.

Usually all observations of the same object within a single FoV crossing constitute a so-called tracklet. A tracklet is a set of observations acquired over short period of time which presumably belong to the same object.

There are several different methods to calculate the information content of a new follow-up tracklet. In this study, the Shannon Information Content (SIC) introduced in [11] is used. Here, the information content is a measure of the reduction of entropy. We suppose S_{before} is the entropy of the knowledge $P(X)$ before and S_{after} is the entropy of the knowledge of $P(X, Y)$ with one additional follow-up tracklet. Then, the SIC is given by:

$$\begin{aligned} SIC &= S_{\text{before}} - S_{\text{after}} \\ &= S[P(X)] - S[P(X, Y)] \end{aligned} \quad (4)$$

If we use the covariance matrix, then finally the SIC is given by:

$$SIC = \frac{1}{2} \ln |P_{\text{pos}}^-| - \frac{1}{2} \ln |P_{\text{pos}}^+| \quad (5)$$

$$= \frac{1}{2} \ln |P_{\text{pos}}^- \cdot (P_{\text{pos}}^+)^{-1}| \quad (6)$$

where $|P_{\text{pos}}^-|$ denotes the determinate of the position covariance matrix before the observation and $|P_{\text{pos}}^+|$ the determinate of the position covariance matrix after the observation. In Fig. 1, an example of the influence on the position error of one additional tracklet during three orbits is shown. Here, a tracklet consists of nine coordinate pairs in azimuth and elevation within two minutes. The propagated position error in radial, along-track and cross-track are represented by dashed lines. If there is a new observation

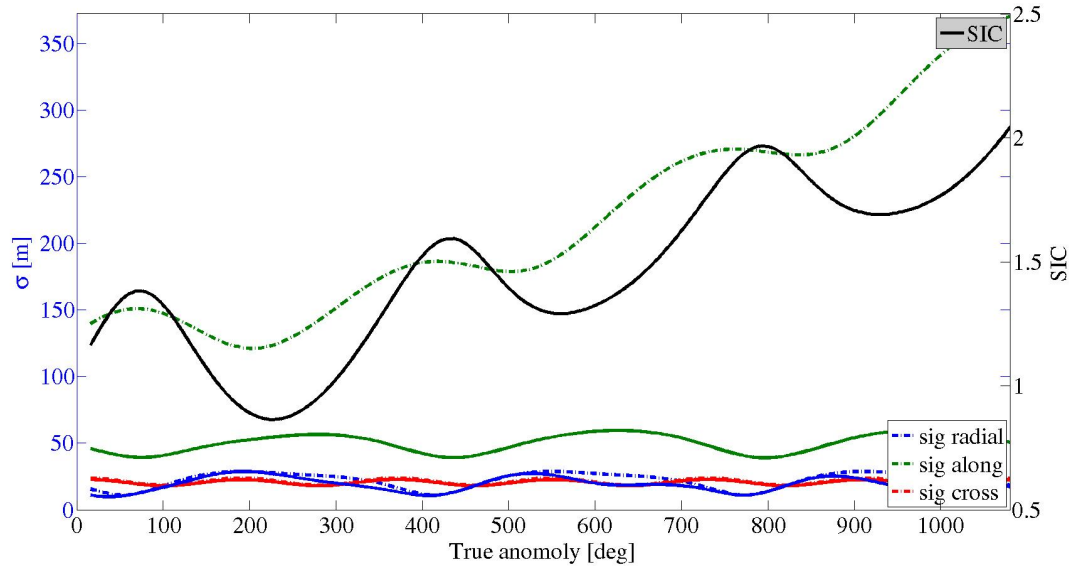


Fig. 1. Evolution of the position error (dashed lines) over three orbits for object 21703. The solid lines represent the improvement of the position error by one new tracklet and the corresponding information content.

tracklet at a specific true anomaly these errors are reduced to a value on the solid line. The information content of each tracklet is represented by the black solid line and follows almost the along-track error line since this error is the major reason for the expansion of the position error ellipsoid. The disadvantage of this method is, that the information content has to be computed for each epoch when the target object could be observed. On the other side, this method ensures that for a given orbit with a corresponding covariance matrix the optimal available observation geometry depending on the observatory and observation time is selected. Illustrating the effect of a single follow-up observation tracklet on the position error in the future, one object from the catalogue (Chapter 3.1) was selected. Starting from the last observation epoch, tracklets with an arc length of 1 min and consisting of five measurements pairs (right ascension and declination) were simulated every 600 s within 24 h. Afterward, the initial orbit at the starting epoch and one simulated tracklet have been used for a new orbit determination and a following orbital propagation over several orbits. In Fig. 2 the position error in along-track direction of some of these propagated orbits are shown. In Fig.2 b the minimum of these error after 10 orbits is shown. The blue dashed line represents the orbit including the optimal scheduled tracklet and reaches a minimum in comparison with the other orbits, which considering tracklets before (red: plus, circle, star, cross) and after (black: square, diamond, pentagram, hexagram) the optimal one.

2.2. Genetic Algorithm

Since scheduling belongs to NP class of problems, heuristics are used to solve this kind of problems. One of the most practical algorithms are the genetic algorithms (GA) inspired by the natural evolution. Their major advantages are the variability to treat any kind of problems and to approximate to solutions for even very complex optimization problems. The high efficiency of these algorithms is reached by the parallel search for solution during each iteration. But this involves also the risk to converge to a non-optimized solution since there is no procedure to develop such a GA. Therefore a lot of tests or simulations, respectively, are required to ensure the capability of the developed algorithm.

Nevertheless, there is a guideline to develop a GA. At the beginning, a population of individuals has to be created. An individual in the sense of GA is a candidate solution to an optimization problem. Based on their fitness, individuals are selected and the two main operators are used to create better solutions. Sometimes it is an advantage to save the solution with the highest fitness value from the previous to the next generation to ensure that there is no worsening. Finally, there have to be criteria to terminate the algorithm. This may be e.g. the number of generations or the highest fitness value.

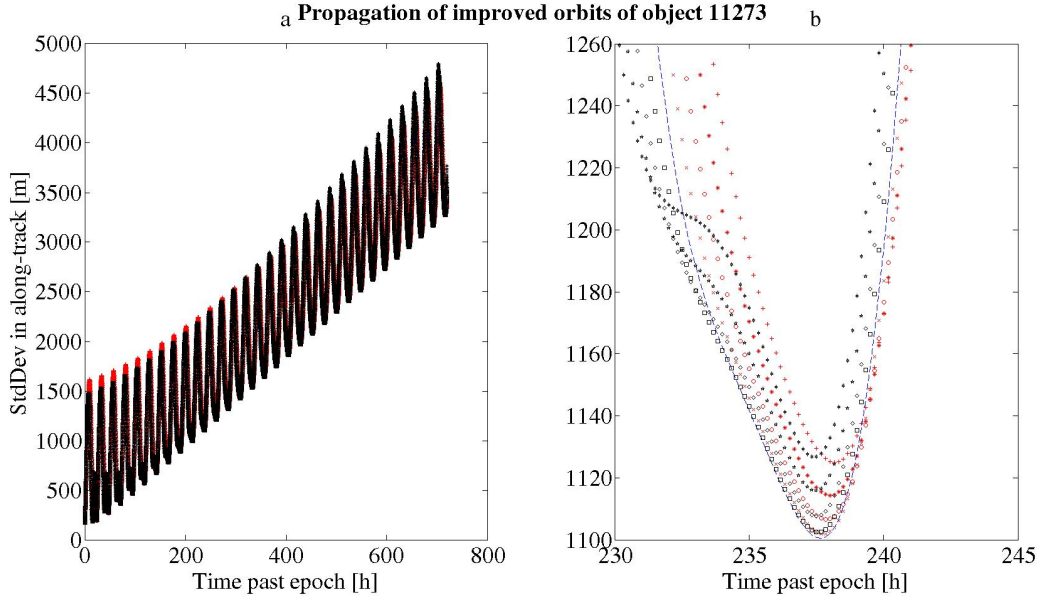


Fig. 2. a) Evolution of the position error in along track over 30 orbits of 11 different determined orbits. Each orbit has the same initial orbit and was updated with one tracklet, which has been simulated at different epochs. b) Evolution of the position error in along track after 10 orbits. The blue dashed line represents the determined orbit using the optimal scheduled tracklet.

Fitness Function The fitness function represents the optimization problem and its solution should be minimized or maximized, respectively. A solution exists for each individual and the determined fitness value allows to compare the solutions. In this study, an individual represents a valid schedule for all telescopes. A valid schedule means, that an observation for each object is scheduled only once and that this object is visible at the given time. Visibility constraints are maximum phase angle, minimum distance to the Moon and to the Earth's shadow, respectively. For the sake of simplicity, it is not possible to schedule an object if one of these conditions is violated. Each scheduled observation of an object j has an expected information content SIC_j at the given time according to Eq. (6). The fitness value F_i of each individual is the sum of all scheduled SIC_j values and is given by:

$$F_i = \sum_{j=1}^N SIC_j \quad (7)$$

Now, the single objective optimization problem is given by:

$$\max F = \max \sum_{j=1}^N SIC_j \quad (8)$$

Initial population An initial population is created at the beginning of each GA. This happens usually randomly to secure a good coverage of the search area. In this study, the number of individuals and therefore the size of the population correspond on the number of chosen objects. Since some objects have the same optimum observation time at the beginning or at the end of the night there is a need to ensure a high diversity of the initial population. Therefore the objects were prioritised by sorting according to their position error. Creating the first individual, the first object (with the worst position error) is chosen and the follow-up observation is scheduled at the optimum time during the night. All other observations were scheduled according to the priority of the object and as close as possible to the optimum time. Thereafter, the first object got the lowest priority. For the second individual, the observation of the new first object was scheduled at the optimum observation time and all other observations again according to the priority of the object. At the end, the object with the highest priority got the lowest one. This procedure was repeated until for each chosen object the observation was scheduled once at the optimum observation time. If more individuals than objects were considered, the remaining individuals were created randomly.

Selection Using Eq. (7), the fitness of each individual is calculated and according to that value individuals are selected for the two main operators in a GA. This allows selecting good solutions for further generations and to eliminate bad solution.

For selection, the rank based selection method was chosen. This method was developed to avoid a early convergence right in the beginning of the search. Instead of using the absolute fitness values of each individual, all individuals are sorted according to their fitness values. Now, the rating of an individual depends on the position only. This ensures that individuals with a high rank are selected with a higher probability in comparison with individuals with a lower rank. Furthermore, this causes also a longer search but increases the probability to find the global optimum. Even if there are many individuals with good fitness values, the selection pressure is still high which avoids to get stuck in the search. Defining the selection probability, Baker [1] suggest following method:

The individual with the highest rank get the expectation values E_{\max} with $1 < E_{\max} < 2$. The expectation values of the worst individual is now given by $E_{\min} = 2 - E_{\max}$. Finally, the expectation values of any other individual is given by:

$$E(a_i) = E_{\min} + (E_{\max} - E_{\min}) \frac{r(a_i) - 1}{n - 1} \quad (9)$$

where $r(a_i)$ is the rank of the individual a_i . The selection probability is then given by

$$p_s(a_i) = \frac{1}{n} E(a_i) \quad (10)$$

Baker suggested the value 1.1 for E_{\max} and this value is also used in the described algorithm. Finally, the selection is performed using stochastic universal sampling with the selection probabilities $p_s(a_i)$. Usually, the number of selected individuals matches the size of the population. Because of the selection probability, some individuals are selected several times and other ones not at all. This leads to the elimination of the worst individuals.

Ensuring that the fittest individual of the next generation is not worse than the fittest one in the current generation, elitism is used and the fittest individual is inserted directly to the next generation. But keep in mind that this individual still may be selected for both crossover and mutation operator, respectively.

Crossover The first operator is the crossover operator which allows big jumps in the search area. Here, two selected individuals are taken and at a given point an interchange occurs. At the end there are two new individuals with properties of the both parent individuals. There are approaches to interchange at a single point or at n-points what depends from the assignment. Finally in most cases a probability is defined when such a crossover may take place.

In the presented algorithms, a random point within a chosen individual is taken. Since each object has to be scheduled only once, an interchange of two objects between the selected individuals might produce a chain of interchanges until each object is scheduled once and both new individuals represents valid schedules. Instead of defining a probability to allow such a crossover, the new individuals are only accepted when their fitness value is better than the average of the whole current population. Otherwise, the parent individuals get to the next generation.

Mutation The second operator used in GA is the mutation which is used to make small jumps in the search area. It is still in discussion which one is more useful but in the end a good balance between crossover and mutations should be guaranteed [8].

In the analyzed scheduling algorithms, a random number of individuals is selected for mutation. For each selected individual, a random number of mutations may take place. At each mutation, a selected observation is interchanged with the observation scheduled before or after the selected one. If this interchange is possible, taking into account the visibility constraints of the object, the sum of $SIC_j + SIC_{j+1}$ is compared to the previous situation. This mutation is accepted if there is an improvement of the fitness.

Final population After performing crossovers and mutations the new population has the same size as the parent population because new individuals were only accepted if there was an improvement of the optimization objective.

2.3. Multiobjective Genetic Algorithm

In some optimization problems, more than one objective has to be optimized. This results, instead of a single optimal solution, in a set of optimal solutions which are also known as Pareto-optimal solutions. Without any further information of the problem, it is not possible to decide which Pareto-optimal solution is better than another one. There are several approaches to deal these solutions and to avoid computational complexity to speed up the algorithms. The most promising approach is described in [2] and is known as NSGA-II. For more detailed information the author refers to [2].

Optimization objective - Magnitude Next to the previous introduced information content of a new measurement the expected magnitude of an object to a given epoch is used as the second optimization objective in the presented multi-objective scheduling algorithm. Especially for faint objects this criterion might increase the detection probability. The apparent magnitude is given by [12]:

$$m_{\text{obj}} = m_{\text{Sun}} - 2.5 \log \left(\alpha \frac{d^2}{4R^2} p_{\text{bond}} p(\Theta) \right) \quad (11)$$

with m_{Sun} the magnitude of the Sun, Lambertian scatterer $\alpha = 1/3$, d the diameter of the object, R the topocentric distance to the object, bond albedo $p_{\text{bond}} = 0.08$, $p(\Theta)$ the phase function with Θ the phase angle. Note that there is no information on the orientation nor change of the orientation considered. Anyway, the apparent magnitude of an observed objects depends directly on the observation geometry

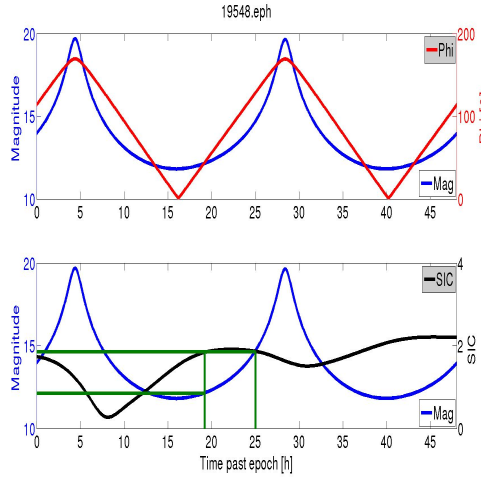


Fig. 3. Top: Evolution of the phase angle and the corresponding magnitude using Eq. (11). Bottom: Evolution of the magnitude and the expected information content of a single observation. The green lines mark epochs for observations with the same information content but different magnitudes.

and therefore on the phase angle. A small phase angle leads to a decreasing magnitude and to a increasing brightness, respectively. Therefore, on the contrary to the information content the phase angle or the magnitude should be minimized. Finally, the magnitude was chosen as the objective parameter since it is less sensitive to small shifts in time. The second fitness function as than given by:

$$\min F = \min \sum_{j=1}^N m_j \quad (12)$$

In Fig. 3 (top), the evolution of the phase angle and the corresponding magnitude is shown. In Fig. 3 (bottom), the evolution of the magnitude and the information content is shown. The delineated green lines highlight that an object might be observed with different magnitudes but the performed measurement has the same information content and therefore the same influence on the orbit improvement. In this case, both objectives can be optimized at the same time.

Non-dominated sorting Usually, optimizing one objective leads to worsening another objective. Therefore, all valid solutions have to be sorted and allocated to one non-dominated front or to a so-called Pareto front, respectively. This requires traditionally, that every solution have to be compared

with all other solution to identify the first non-dominated front. Excluding these solutions, all remaining solutions have to be compared again to find the following non-dominated front and so on. Finally, this requires in the worst case of N fronts and N solutions a computation complexity of $O(MN^3)$ where M is the number of objectives. In Fig. 4, a scheme of non-dominated fronts for two minimization functions is shown. In [2], a fast non-dominated procedure is introduced which reduces the computation complexity to $O(MN^2)$ by using n_p , which counts the number of solution which dominate solution p and the set S_p which includes all solutions that are dominated by solution p . This procedure is used in this study.

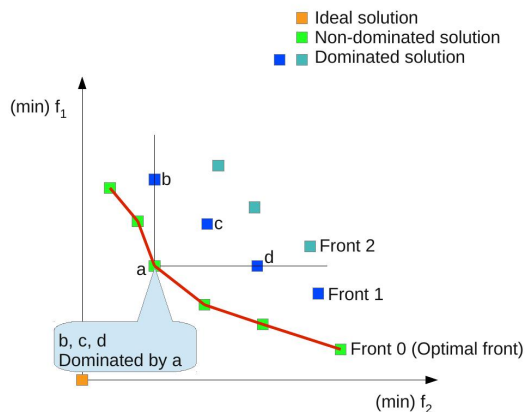


Fig. 4. Scheme of the Pareto fronts for a bi-objective minimization problem.

Crowding distance assignment As mentioned above, without any further information it is not possible to say which solution is better than the other one within one non-domination front. Therefore, a mechanism called crowding distance was developed. Here, the density of solutions around a particular solution in one front is estimated. In this study, an improved mechanism is used. This mechanism is introduced in [3] and avoids the instability if several solutions share the same fitness.

Initial population On the contrary to the GA, where all individuals are sorted according to their fitness, here all initial individuals are allocated to Pareto fronts using the non-dominated sorting procedure. Afterward, all individuals in one front are sorted according to their crowding distance and the selection procedure can start.

Final population After performing crossovers and mutations, the new child population has the same size as the parent population. All $2N$ solutions are sorted using the non-dominated sorting and the crowding distance procedure. After that the first N solutions are saved as the final population and used as input for the next generation.

3. RESULTS

Simulations were used to demonstrate the functionality to schedule observations according to their information content (both algorithms) and the magnitude (only MOGA). Further, the effectivity of the GA and MOGA is illustrated and compared.

3.1. Catalogue

Base for the simulated small size space debris object catalogue is the USSTRATCOM catalogue from 2016-01-01. This USSTRATCOM catalogue was taken to ensure a realistic distribution of the orbital elements. Using the ranges of the orbital elements given in Tab. 1, 762 objects were selected to simulate observations from the observatory in Sutherland, (South Africa) between 2016-01-01 and 2016-02-10. For each of these objects, a random number of observation nights within the campaign was chosen, whereas a minimum of 10 observation nights was required. On every observation night one tracklet was simulated, consisting of 10 observations with an arc length of two minutes. All observations have a standard deviation of $2''$. Furthermore, an area-to-mass ratio value (AMR) Gaussian distribution with

$\text{mean}_{\text{AMR}} = 0.02 \text{ m}^2 \text{ kg}^{-1}$ and $\sigma_{\text{AMR}} = 3.0 \text{ m}^2 \text{ kg}^{-1}$ (only positive values considered) was simulated. For simplification, the magnitudes were assigned proportional to the AMR values by assuming a constant mass of 10 kg.

Tab. 1. Orbital elements

$35\,000 \text{ km} \leq a < 50\,000 \text{ km}$
$0.0 \leq e < 0.3$
$0.0^\circ \leq i < 20.0^\circ$
$0.0^\circ \leq \Omega < 360.0^\circ$
$0.0^\circ \leq \omega < 360.0^\circ$
$0.0^\circ \leq M < 360.0^\circ$

3.2. Simulation environment

In the used version of the scheduling algorithms, the visibility of each object was limited by a minimum elevation of 20° above the horizon. Taking the allocated AMR values of the objects, a limited sensor sensitivity of 17 magnitude was considered. Furthermore, a minimum distance of 20° to the Moon and galactic plane, respectively, were required to allow the scheduling of an object. Simulations were performed for the telescope in Sutherland (South Africa) (see Tab. 2).

Tab. 2. Telescope location:
Longitude λ , Latitude φ and Height h

	$\lambda[^\circ]$	$\varphi[^\circ]$	$h[\text{m}]$
Sutherland	20.813	-32.937	1700

3.3. Performance of the Genetic Algorithm

During the night of 2016-02-15 at the observatory in Sutherland a total observation time of 533 min was available and 182 objects could be observed. Simulations were used to determine the optimal configuration regarding to the number of individuals and generations. Finally, good results were reached if the number of individuals is equal to the maximum number of objects to schedule per telescope. This ensures on the one hand, that each object was scheduled once at the optimum epoch at the beginning (initial population) and on the other hand it reduces the number of crossover and mutations. Nevertheless, the algorithm scheduled all objects within a processing time of 3 min.

Fig. 5 shows the results of five runs. Each colour represents one run of the GA with randomly chosen positions for crossover and mutation. On the left hand side (Fig. 5a) the average of the information content values is shown. The fluctuation at the beginning is caused by the increasing number of objects which could be scheduled during the processing. On the right hand side (Fig. 5b) the average of the magnitude values is shown. Note, that using the GA, this values was not optimized. The average values were selected to compare the different simulations performing the GA and MOGA. Finally, after about 500 generations the algorithm converged to the optimum and therefore the optimized schedule was created. Furthermore, statistics of the differences between the optimal values and the scheduled ones for the information content and the magnitudes, respectively, are shown in Fig. 6. Most of the objects were scheduled close to their optimal epoch ensuring a high information content of the measurement. On the contrary, the statistic for the magnitude is worse since it was not optimised.

3.4. Performance of the Multi-objective Genetic Algorithm

The same conditions like in the previous case performing the GA are used to illustrate the performance of the MOGA. The implemented algorithm scheduled all objects within a process time of about 90 s. On the contrary to GA, simulation showed good results using a population size of $2N$ while considering N objects to schedule for one telescope. Illustrating the performance of the used MOGA, the results of five runs (represented by different colours) are shown in Fig. 7. On the left hand side the evolution of the average information content is shown, whereas on the right hand side the evolution of the average magnitudes is shown. After about 500 generations the algorithms converges by finding the final solution with the best

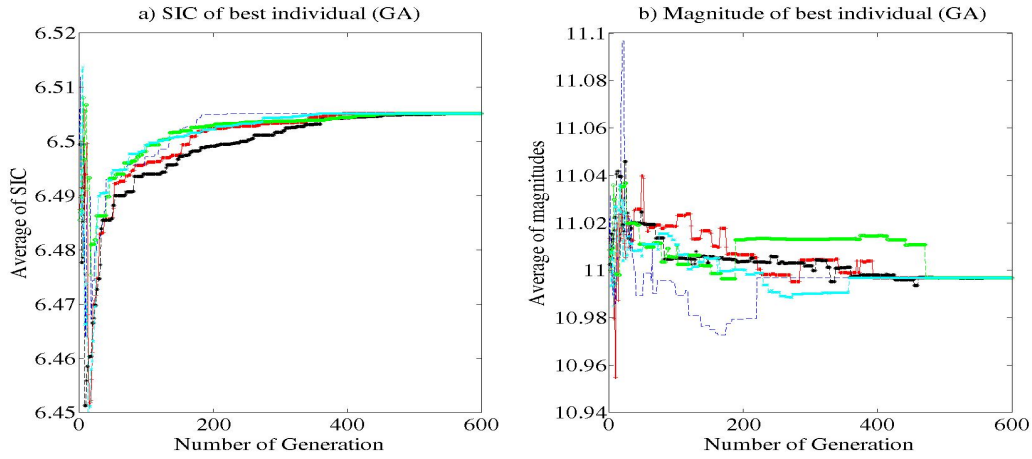


Fig. 5. Convergence of the GA finding the optimum solution scheduling observations for 182 objects for the telescope in Sutherland. Each colour represents a run of the GA using random positions for crossover and mutation operator, respectively. a) Optimised information content b) non-optimised magnitudes.

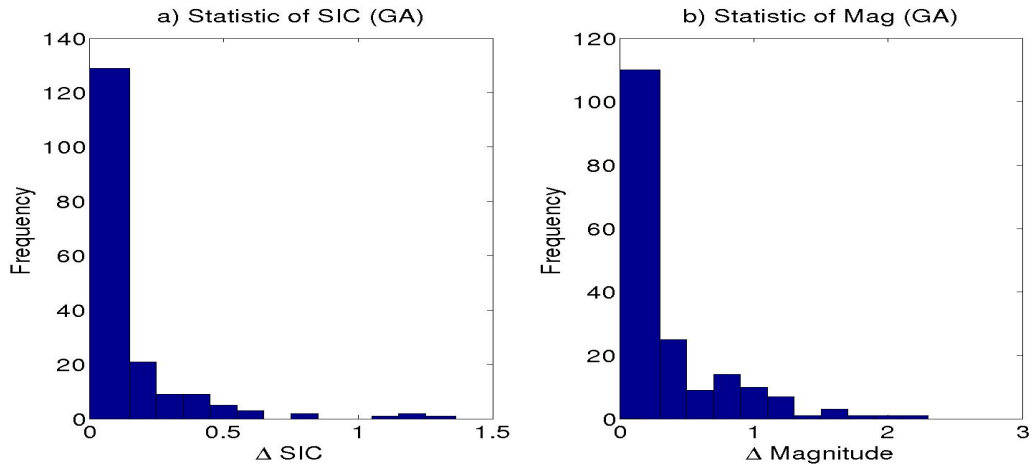


Fig. 6. Statistics of the differences between the optimal values and the scheduled one performed by GA using the telescope in Sutherland. a) Information content b) Magnitudes

rank and highest crowding distance during the next generations. The fluctuation at the beginning of the scheduling process are caused by an increasing number of objects which could be scheduled. Afterward, the algorithm was oscillating between both objectives with a constant number of scheduled objects.

Fig. 8 shows the statistics of the differences between the optimal values and the scheduled ones for the information content and the magnitudes, respectively. In comparison with the results of the GA (Fig. 6), on the one hand more objects were scheduled closer to their optimal information content values (Fig. 8a) and on the other hand the distribution is reduced. A reduced distribution of the differences in the magnitudes are also shown in Fig. 8b in comparison with the results of the GA. But using the GA, more objects are scheduled closer to their optimal magnitudes what might be a hint, that the magnitude may be not a good optimization objective. Finally, in Tab. 3 the statistical values are summarised.

Tab. 3. Statistical results.

Name	Mean _{SIC}	σ_{SIC}	Mean _{Mag}	σ_{Mag}
GA	0.1464	0.2228	0.3625	0.4382
MOGA	0.0819	0.1017	0.4167	0.4133

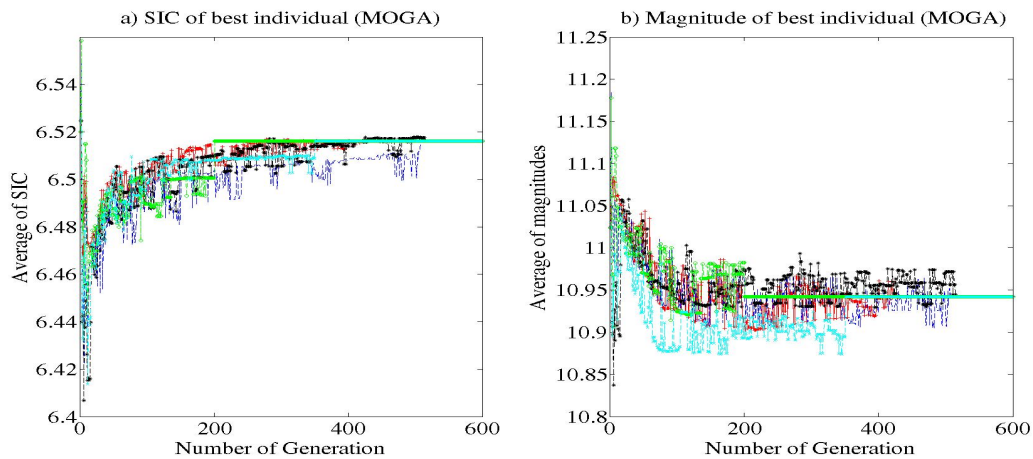


Fig. 7. Convergence of the MOGA finding the optimum solution scheduling observations for 182 objects for the telescope in Sutherland. Each colour represents a run of the GA using random positions for crossover and mutation operator, respectively. a) Optimized information content b) Optimized magnitudes.

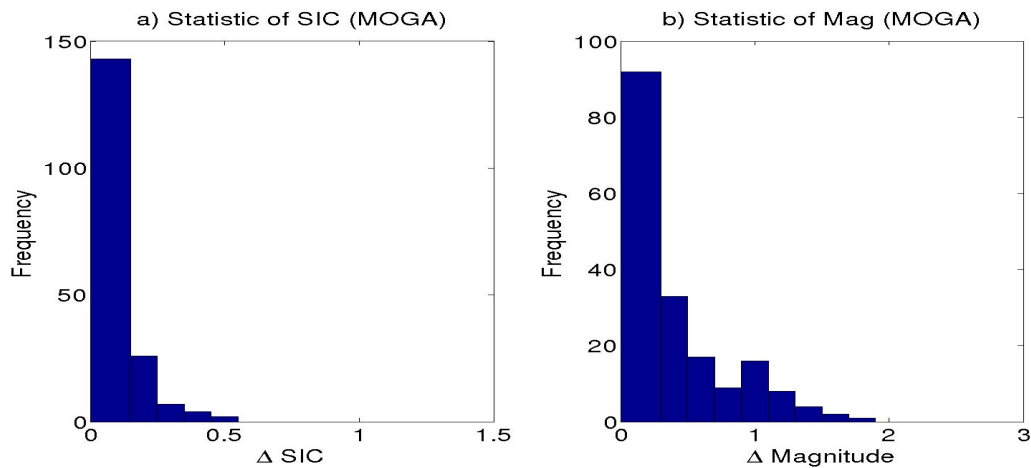


Fig. 8. Statistics of the differences between the optimal values and the scheduled one performed by MOGA using the telescope in Sutherland. a) Information content b) Magnitudes

4. CONCLUSION

In this work, two optimized scheduling algorithms were introduced and compared. The first optimization objective, the information content of a follow-up tracklet was used in both algorithms and based on its influence to reduce the position error covariance. This reduction depends on the used observatory, the time of the observation and the previous determined covariance of the object. Scheduling observations corresponding to this information content may minimize the number of necessary follow-up observations for catalogue maintenance. The results of the GA show that all required observations of the selected objects are scheduled and that the genetic algorithm converges to an optimum. Using random positions for crossover and mutation operators, the algorithm converges after about 600 generation to the maximum. Improving the performance of the scheduled observation, the GA was expanded to a multi-objective genetic algorithm. As the second optimization parameter the magnitude at the observation epoch was estimated. Especially faint objects have to be observed at low phase angles whereby the magnitude decreases and therefore the detection probability increases. It has been shown that some observations with different magnitudes might have the same information content and therefore the same influence on the orbit improvement. In these cases the algorithm may optimize both objectives. The results of the MOGA show, that even taking the double number of individuals a comparable number of generations is needed to converge. Finally, better results for the information content values were reached. Considering the magnitude as the second optimization objective no improvement was apparent. Here, a further

analysis have to be performed. Finally, comparable to the GA the MOGA converges between 400 and 500 generations.

ACKNOWLEDGEMENT

The work was funded by the Munich Aerospace scholarship program. The author would like to thank Johannes Herzog for his continuous support throughout this research.

5. REFERENCES

1. J. E. Baker. Adaptive Selection Methods for Genetic Algorithms. In *Proceedings of an International Conference on Genetic Algorithms and their Applications*, 1985.
2. K. Deb. A Fast and Elitist Multiobjective Genetic Algorithm: NSGA-II. *IEEE Transactions on Evolutionary Computation*, (6):182 – 197, 2002.
3. A. Fortin, F. and M. Parizeau. Revisiting the NSGA.II Crowding Distance Computation. In *Proceedings of the 15th annual conference on Genetic and evolutionary computation*, 2013.
4. J. Herzog. *Cataloguing of Objects on High and Intermediate Altitude Orbits*. Phd thesis, University of Bern, November 2013.
5. J. Herzog, H. Fiedler, M. Weigel, O. Montenbruck, and T. Schildknecht. Smartnet: A Sensor for Monitoring the Geostationary Ring. In *Proceedings of the 24th International Symposium on Space Flight Dynamics*, 2014.
6. K. Hill, P. Sydney, K. Hamada, R. Cortez, K. Luu, M. Jah, P.W. Schumacher, M. Coulman, J. Houchard, and D. Naholoewa. Covariance-Based Network Tasking of Optical Sensors. In *Proceedings of the Space Flight Mechanics Conference*, 2010.
7. K. Hill, P. Sydney, K. Hamada, R. Cortez, K. Luu, M. Jah, P.W. Schumacher, M. Coulman, J. Houchard, and D. Naholoewa. Covariance-Based Scheduling of a Network of Optical Sensors. In *AAS/AIAA Kyle T. Alfriend Astrodynamics Symposium*, 2010.
8. M. Mitchell. *An Introduction to Genetic Algorithms*. The MITT Press, Cambridge and London, 1996.
9. S. Moisan, M. Boer, C. Thiebaut, F. Tricoire, and M. Thonnat. A Vertisale Scheduler for Automatic Telescopes. In *Proceedings of the SPIE Conference on Astronomical Instrumentation and Methods*, 2002.
10. R. Musci, T. Schildknecht, and M. Ploner. Orbit Improvement for GEO Objects Using Follow-up Observations. *Advances in Space Research*, (34):912 – 916, 2004.
11. C. D. Rodgers. *Inverse Methods of Atmospheric Sounding, Theory and Practice*. 2000.
12. Thomas Schildknecht. *The Search for Space Debris in High-altitude Orbits*. Habilitation thesis, University of Bern, November 2003.